Original Article

Identifying biomarkers associated with tumor growth rate: a longitudinal preoperative magnetic resonance imaging follow-up of low-grade gliomas

Yukun Liu[1,2], Ziwen Fan[1], Shaowu Li[3], Xing Liu[4], Tao Jiang[1,2], Yinyan Wang[1,5], Lei Wang[1]

[1]Department of Neurosurgery, Beijing Tiantan Hospital, Capital Medical University, Beijing, China; [2]Beijing Neurosurgical Institute, Capital Medical University, Beijing, China; [3]Department of Neuroradiology, Beijing Tiantan Hospital, Capital Medical University, Beijing, China; [4]Department of Pathology, Beijing Tiantan Hospital, Capital Medical University, Beijing, China; [5]China National Clinical Research Center for Neurological Diseases, Beijing, China

Contributions: (I) Conception and design: Y Wang, L Wang, T Jiang; (II) Administrative support: Y Wang, L Wang, T Jiang; (III) Provision of study materials or patients: Y Liu, Z Fan, S Li, X Liu; (IV) Collection and assembly of data: Y Liu, Z Fan; (V) Data analysis and interpretation: Y Liu, Z Fan; (VI) Manuscript writing: All authors; (VII) Final approval of manuscript: All authors.

Correspondence to: Yinyan Wang. Department of Neurosurgery, Beijing Tiantan Hospital, Capital Medical University, 119 South Fourth Ring West Road, Fengtai District, Beijing 100070, China. Email: tiantanyinyan@126.com; Lei Wang. Department of Neurosurgery, Beijing Tiantan Hospital, Capital Medical University, 119 South Fourth Ring West Road, Fengtai District, Beijing 100070, China. Email: wanglei_tiantan@163.com.

Background: Although the influence of molecular biomarkers on the biological behavior of tumor cells has been investigated, their quantitative influence on the velocity of tumor growth remains unclear. This study aimed to identify the molecular biomarkers associated with tumor growth rates in World Health Organization (WHO) grade II gliomas, or low-grade gliomas (LGGs).

Methods: Preoperative magnetic resonance imaging (MRI) data of patients with LGGs were retrospectively reviewed. Patients with at least 2 preoperative MRIs taken more than 90 days apart were enrolled. Patients with isocitrate dehydrogenase (*IDH*) wild-type tumors or with no recorded *IDH* status were excluded. A linear mixed-effects model was used to assess the velocity of tumor diameter expansion. The effect of biomarker expression on tumor growth rate was assessed using a multivariate linear mixed-effects regression model.

Results: Data from 56 patients were used in our study. The overall velocity of diameter expansion (VDE) for LGGs was 2.1 mm/year. Higher expression level of mutant p53 were significantly associated with a higher tumor growth rate (+1.9 mm/year, P<0.01), while higher expression level of alpha-thalassemia/mental retardation syndrome X-linked protein (ATRX) were significantly associated with a lower tumor growth rate (–1.3 mm/year, P<0.01). Tumors with O6-methylguanine-DNA methyltransferase (*MGMT*) promoter methylation were found to grow significantly more slowly than those with no methylation (–3.1 mm/year, P<0.01). The telomerase reverse transcriptase (*TERT*) promoter type and expressions levels of Ki-67 and epidermal growth factor receptor (EGFR) showed no significant independent impact on tumor growth rates.

Conclusions: The status of biomarkers is significantly associated with the tumor growth rate in LGGs.

Keywords: Glioma; magnetic resonance imaging; biologic markers

Submitted Aug 05, 2021. Accepted for publication Feb 08, 2022.
doi: 10.21037/atm-21-3998
View this article at: https://dx.doi.org/10.21037/atm-21-3998

Introduction

Low-grade gliomas (LGGs) are brain tumors that generally grow linearly and infiltrate diffusely (1,2). Although most LGGs are indolent, their clinical behavior is highly variable and cannot be adequately predicted based on their histologic class (3). Molecular examination has become an important part of glioma diagnosis, and many diffuse astrocytomas with wild-type isocitrate dehydrogenase (*IDH*)—previously considered low-grade tumors—which may be more likely to progress aggressively, are now classified as World Health Organization (WHO) grade 4 tumors (4). Although complete neurosurgical resection of LGGs is sometimes impossible, maximum safe resection remains the goal of management of LGG, which also involves clinical monitoring, chemotherapy, and radiotherapy, and depends on the histological type and molecular subtype of the tumor and the clinical status of the patient (5).

The tumor growth rate directly reflects the biological characteristics of gliomas during their natural growth process. Fast-growing gliomas should be treated immediately, and timely examinations should be performed after surgery. Radius or diameter measurements of LGGs reveal linear growth, and the velocity of diameter expansion (VDE) is generally used as a quantitative indicator of the tumor growth rate (1,2,6). The VDE is an independent prognostic factor in patients with gliomas (7-9) and has been used to assess the effectiveness of treatments such as chemotherapy (10-12) and radiotherapy (11,13). The VDE is also considered a quantitative indicator of tumor malignancy (7,8). Compared to patient survival time, VDE better reflects the characteristics and invasiveness of the tumor itself, as it prevents clinical treatment factors, such as the extent of resection or any adjuvant therapy, from influencing the results obtained (14,15).

Molecular biomarkers play an important role in determining the biological behavior of gliomas and the survival time of patients (5,16). Mutant p53 protein overexpression has been shown to accelerate LGG growth rates (8), while 1p/19q codeletion has been shown to significantly decelerate LGG growth rates (9,10,14). In contrast, *IDH1* variations are considered to have no significant influence on tumor growth (8,9,17). Although the influence of molecular biomarkers on the biological behavior of tumor cells has been investigated (18-21), their quantitative influence on the velocity of tumor growth remains unclear.

Only a few longitudinal studies have obtained multiple magnetic resonance (MR) scans of tumors prior to surgery (1,2,8-10,12-14,22-24). Hence, the factors that influence the natural development of LGGs are still unclear. Additionally, inconsistent results regarding the growth rate of LGGs have been reported. The present study systematically investigated the effects of molecular biomarker status on the natural growth rate of gliomas. We analyzed the following molecular biomarkers that determine the classification of adult diffuse glioma in the 2021 WHO classification of tumors of the central nervous system (4) and those recommended by the Chinese Glioma Cooperative Group (CGCG) guidelines on tumor growth, since they help define the biological and clinical behavior of gliomas (5): alpha-thalassemia/mental retardation, X-linked (ATRX), telomerase reverse transcriptase (*TERT*), epidermal growth factor receptor (EGFR), mutant p53, Ki-67, O6-methylguanine-DNA methyltransferase (*MGMT*), and 1p/19q. We present the following article in accordance with the REMARK reporting checklist (available at https://atm.amegroups.com/article/view/10.21037/atm-21-3998/rc).

Methods

Patient selection

Clinical information and imaging data from patients who underwent primary surgical treatment between January 2008 and October 2021 and were pathologically diagnosed with LGGs were retrospectively reviewed (*Figure 1*). The patient inclusion criteria were as follows: (I) diagnosis at age ≥18 years; (II) 2 or more magnetic resonance imaging (MRI) examinations before surgery; (III) no chemotherapy or radiotherapy received prior to surgery; and (IV) histologically confirmed WHO grade II glioma. Due to the value of the patient's *IDH* status in diagnosing LGGs, patients with an *IDH* wild-type tumor or with no recorded *IDH* status were excluded. To avoid bias, patients for whom sequential MRIs were performed at intervals of less than 90 days were excluded from this study. A total of 56 patients with LGGs were finally included. The study was conducted in accordance with the Declaration of Helsinki (as revised in 2013). The study was approved by the ethics committee of Beijing Tiantan Hospital (No. KYSB2016-026) and as a retrospective study, all clinical information was collected from the institutional medical database, therefore individual

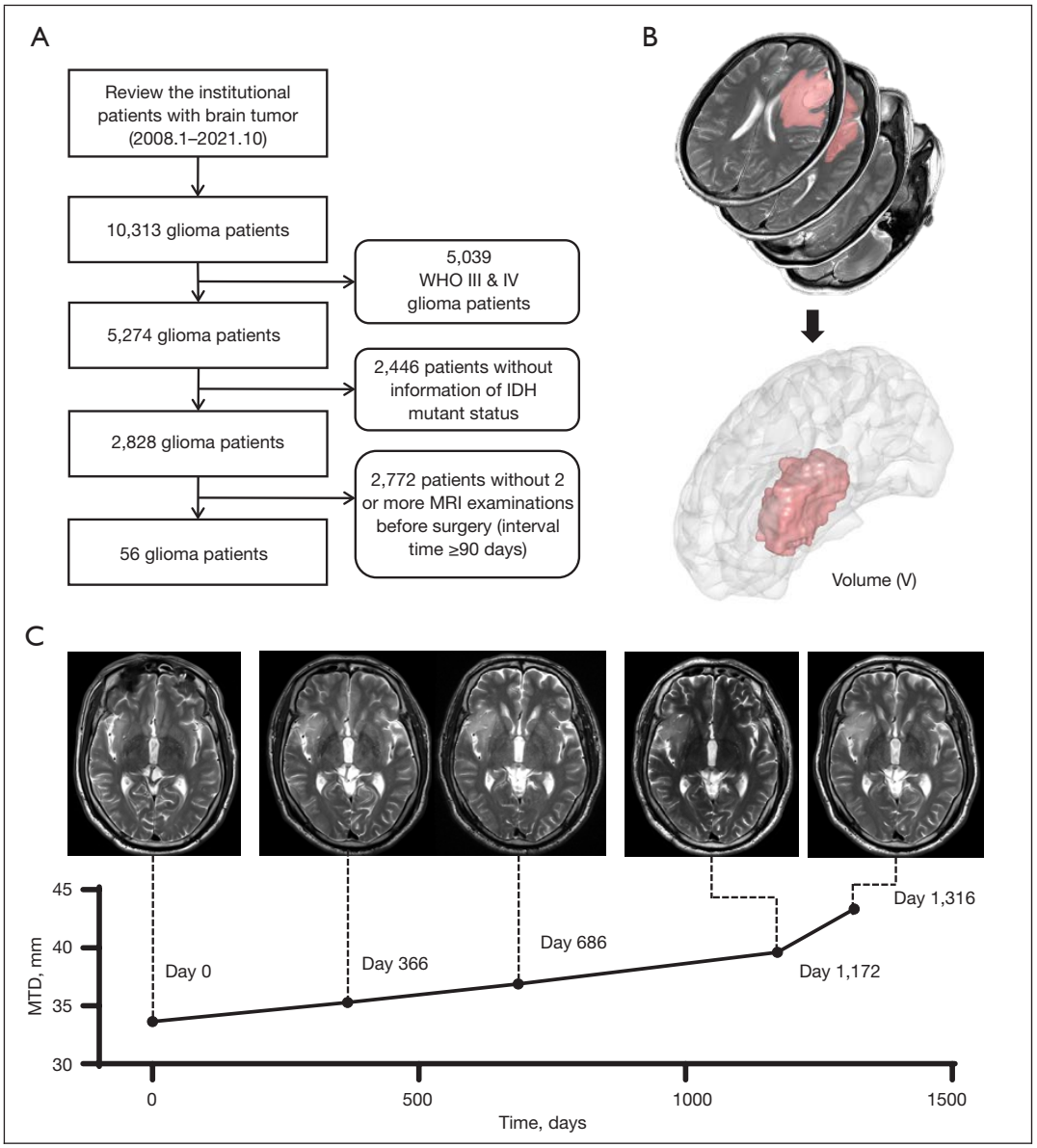

Figure 1 Workflow diagram. (A) Process of patient inclusion. (B) Measurement of the tumor volume. Tumor volume was calculated as layer thickness × tumor region of interest and converted to MTD using the formula: $MTD = (2\times V)^{1/3}$. (C) shows the curve of a patient's MTD over time. IDH, isocitrate dehydrogenase; MTD, mean tumor diameter; WHO, World Health Organization; MRI, magnetic resonance imaging.

consent for this retrospective analysis was waived.

MRI data acquisition

A Magnetom Trio 3T scanner (Siemens AG, Munich, Germany) was used to acquire all MRI scans. The T2-weighted imaging parameters were as follows: repetition time =5,800 ms; echo time =110 ms; flip angle =150 degrees; 24 slices; field of view =240×188 mm^2; and voxel size =0.6×0.6×5 mm^3. The brain lesions of each patient were manually segmented by 2 board-certified neurosurgeons using the free access software MRIcro (http://www.mccauslandcenter.sc.edu/mricro/) and re-evaluated by a neuroradiologist with over 20 years of experience in tumor diagnosis. When there was a discrepancy exceeding 5% between the neurosurgeons, a senior neuroradiologist

determined the lesion border (25).

Assessment of molecular biomarkers

The expression levels of ATRX, EGFR, mutant p53, and Ki-67 were examined in tumor tissue by immunohistochemistry (IHC), following the procedure introduced in our previous studies (26-28). Staining was scored on a 5-point scale from 0 to 4, where 0 = no or rare occurrence of staining; 1 = 10% of cells stained positively; 2 = 10–30% of cells stained positively; 3 = 30–60% of cells stained positively; and 4 = 60% or more of cells stained positively. Following our previous study (29), *IDH* variations were identified using DNA pyrosequencing, *TERT* promoter variational status was determined using Sanger sequencing, and 1p/19q codeletion status was detected by fluorescence *in situ* hybridization (FISH). The *MGMT* promoter methylation status was determined by methylation-specific polymerase chain reaction (PCR) after sodium bisulfite DNA modification, as described previously (30). A dichotomous classification method was used to obtain the subgroups for each biomarker according to the different expression levels or variation statuses. The final cutoff of expression levels of each biomarker examined by IHC is shown in Table S1.

Tumor growth model

Most studies quantitatively measuring tumor growth rates have used a linear growth model (1,8-10,12-14,23,24). Since it is not affected by the initial volume, a linear model can intuitively observe the differences in growth rates between different subgroups. Therefore, we chose the linear growth model to analyze the influence of different factors on tumor growth rates. Changes in tumor size are represented by the change in mean tumor diameter [MTD; $MTD = (2 \times V)^{1/3}$] (15) over time, and the tumor volume (V) was calculated using MATLAB (version 2014a, The MathWorks, Natick, MA, USA) based on the voxels of the segmented tumor region on T2-weighted images (*Figure 1*). The VDE was estimated using linear regression for diameter expansion for each case. To examine the overall tumor growth trend of the dataset, we used an improved linear mixed-effects model (LMEM) with a fixed slope unlike that used in previous studies (1,31) and calculated the equivalent VDE (eVDE) using the following formula:

$$MTD_{ij} = \mu + \alpha_{1i} + \beta_1 \times T_{ij} + \beta_2 \times IMTD_i + \varepsilon_{ij} \quad [1]$$

where MTD_{ij} denotes the MTD for patient i at the time of observation j; β_1 represents the eVDE and is the slope of the regression line of the LMEM; $\mu + \alpha_{1i}$ is the intercept for patient i; T_{ij} represents the time of observation j for patient i; $IMTD_i$ is the initial MTD of patient i; β_2 is the fixed effect of $IMTD_i$; and ε_{ij} is the residual term.

To describe the differences in tumor growth rates based on the status of each factor, such as the high or low expression level of a biomarker, a multivariate LMEM model (mLMEM) with an interaction term was used as follows:

$$MTD_{ij} = \mu + \alpha_{1i} + \beta_1 \times T_{ij} + \beta_2 \times IMTD_i + \beta_3 I_{ik} + \beta_4 T_{ij} \times I_{ik} + \varepsilon_{ij} \quad [2]$$

where MTD_{ij}, $IMTD_i$, T_{ij}, $\mu + \alpha_{1i}$, β_1, β_2, and ε_{ij} are as defined above; β_3, and β_4 are fixed effect coefficients; I_{ik} represents patient i in the kth status of factor I; $T_{ij} \times I_i$ is the interaction term of time and factor; and its coefficient β_4 represents the effects of factor I on tumor growth rate. Thus, the regression lines of the LMEM for gliomas that differ in factor I status can be compared quantitatively, and the interaction effects on tumor growth rate can be identified.

Statistical analyses

We included gender, age, and histological classification as clinical factors. The interaction effects of the clinical factors and time were analyzed using mLMEM. Age was used as a continuous variable, while gender, histological classification, and molecular expression status were included as categorical variables in the analysis model. We also calculated the effects of different factor statuses on the tumor growth rate (using mLMEM). The Akaike information criterion, Bayesian information criterion (BIC), R^2 coefficient, R^2-adjusted, and mean square error were used to evaluate the model. In addition, the tumor growth rate in all patients, or a single patient, and its 95% confidence interval (CI) were calculated using LMEM. A P value ≤0.05 was considered statistically significant. To avoid bias caused by missing data, we first evaluated the interaction effects of missing data to determine if the presence or absence of data for a biomarker created distribution inconsistencies between the subgroup with missing data and the subgroup with complete data. Only biomarkers with consistent distribution (for which the interaction effect was not significant) were incorporated in multivariable analysis.

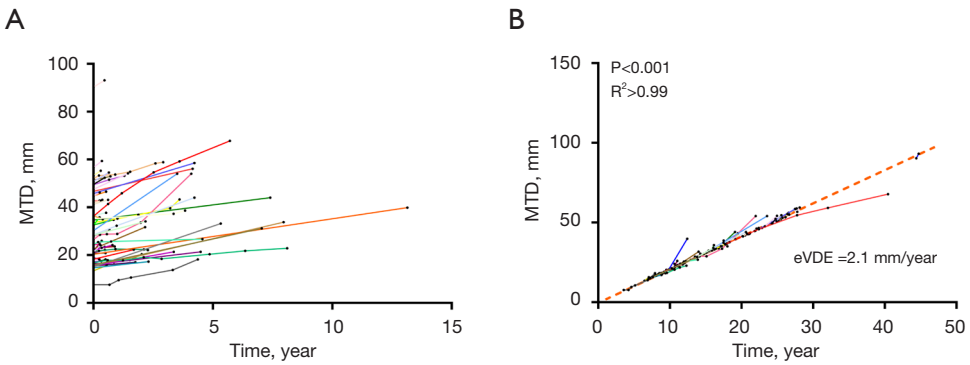

Figure 2 Tumor growth curve of each patient and the eVDE fitted by a LME. (A) The evolution of the MTD over time for each patient. (B) The eVDE of each patient. An LMEM was used to describe the trend in overall tumor growth before surgery. The slope of the LMEM regression line representing the eVDE was 2.1 mm/year in 56 patients with LGGs (95% CI: 1.8 to 2.4 mm/year, P<0.001, R^2>0.99; orange dotted line). eVDE, equivalent velocity of diameter expansion; LME, linear mixed model; MTD, mean tumor diameter; LMEM, linear mixed-effects model; LGG, low-grade glioma; CI, confidence interval.

Results

Patient demographics

The data from a total of 56 patients (39 males and 17 females) were used in this study. The median age at the time of tumor detection on the first MRI examination was 36 years (range: 21 to 62 years). The median interval between the first MRI and preoperative MRI examination was 472 days (range: 91 to 4,799 days). The median tumor volume at the first detection was 9.4 cm^3 (range: 0.2 to 368.0 cm^3), and that at the last examination before surgery was 19.8 cm^3 (range: 1.9 to 404.1 cm^3). The growth curve of each patient and the regression lines for all patients are shown in *Figure 2*.

The VDE and clinical factors

For the 56 patients, the mean VDE was 3.3 mm/year, and the median VDE was 2.6 mm/year; the eVDE was 2.1 mm/year (95% CI: 1.8 to 2.4 mm/year, P<0.001, R^2>0.99) (*Figure 2*). The influence of clinical characteristics on the tumor growth rate was assessed using mLMEMs (*Table 1*). Female patients were found to have a significantly higher eVDE than male patients (2.6 *vs.* 1.9 mm/year, P=0.02). Age was found to have a significant influence on eVDE (P<0.01). When the age at the first radiological diagnosis of LGGs increased by 1 year, the eVDE slowed by 0.05 mm/year. Among patients who could be clearly classified under the 2021 WHO classification, those with diffuse astrocytoma, *IDH* mutant-type exhibited significantly faster tumor growth than those with oligodendroglioma, *IDH* mutant-type (3.4 *vs.* 1.4 mm/year, P<0.01).

Effects of biomarker status on eVDE

The influence of the molecular biomarkers on the eVDE was assessed using mLMEMs (*Table 2*). High expression level of p53 were found to be significantly associated with a high eVDE (high expression, 4.5 mm/year *vs.* low expression, 1.5 mm/year; P<0.01), as were high expression level of EGFR (high expression, 4.0 mm/year *vs.* low expression, 2.2 mm/year; P<0.01).

A low eVDE was found to be significantly associated with *TERT* promoter type (mutant, 1.6 mm/year *vs.* wild-type, 3.4 mm/year; P<0.01), the 1p/19q codeletion status (codeletion, 1.4 mm/year *vs.* non-codeletion 3.4 mm/year; P<0.01), the *MGMT* promoter methylation status (methylation, 2.0 mm/year *vs.* non-methylation, 5.0 mm/year; P<0.01), high expression level of ATRX (high expression, 1.1 mm/year *vs.* low expression, 3.6 mm/year; P<0.01), and high expression level of Ki-67 (high expression, 1.9 mm/year *vs.* low expression, 2.6 mm/year; P=0.05).

Multiple-factor analysis using mLMEM

The interaction effects of missing data for different biomarkers are shown in Table S2. The presence or absence of EGFR and *TERT* promoter data caused significant

Table 1 Clinical characteristics of patients and their effects on the eVDE

Characteristic	N/value	eVDE (mm/year)	Estimated effects (mm/year ± SE)	P value
Gender				
Male	39	1.9	0.8±0.3	0.02*
Female	17	2.6		
Age in years, median [range]	36 [21–62]		−0.05±0.01	<0.01*
Histological classification				
Diffuse astrocytoma, IDH mutant-type	21	3.4	−2.1±0.3	<0.01*
Oligodendroglioma, IDH mutant-type	19	1.4		
Diffuse astrocytoma, NOS	4	3.3	–	–
Oligodendroglioma, NOS	4	1.7	–	–
Oligoastrocytoma, NOS	8	2.8	–	–
Initial mean tumor diameter in cm, median (range)	2.7 (0.8–9.0)			
Initial tumor volume in cm^3, median (range)	9.4 (0.2–368.0)	–	–	–
Preoperative tumor volume in cm^3, median (range)	19.8 (1.9–404.1)	–	–	–
Interval time between MRIs in days, median (range)	472 (91–4,799)	–	–	–
Number of available MRIs, average [range]	2.6 [2–8]	–	–	–

*, a P value ≤0.05 was considered statistically significant. eVDE, equivalent velocity of diameter expansion; IDH, isocitrate dehydrogenase; MRI, magnetic resonance imaging; SE, standard error.

distribution inconsistencies, and both the group with missing data and the group with complete data were excluded from the model. Histological classifications determined by biomarkers were also excluded. We used Ki-67, mutant p53, 1p/19q, ATRX, *MGMT* promoter, age, and gender as interaction terms in the mLMEM to assess whether they were independent influencing factors. In the multiple-factor analysis, age (P<0.01), expression levels of mutant p53 (P<0.01) and ATRX (P<0.01), and *MGMT* promoter methylation (P<0.01) had a significant impact on the eVDE (*Table 3*, *Figure 3*).

The estimated effect of factors on the diffuse astrocytoma, *IDH* mutant-type and oligodendroglioma, *IDH* mutant-type subgroups were also analyzed by multiple-factor analysis (*Table 4*). Age, expression levels of mutant p53, and *MGMT* promoter methylation were independent factors that influenced tumor growth rates in the diffuse astrocytoma, *IDH* mutant-type subgroup, while age and gender were independent factors that influenced tumor growth rates in the oligodendroglioma, *IDH* mutant-type subgroup.

Discussion

Tumor growth rate is considered to directly reflect the characteristic natural malignancy of a tumor and its invasiveness in the absence of the influence of clinical treatment. The genetic background of gliomas has been hypothesized to influence the tumor growth rate (10,14). The current study quantitatively investigated whether the status of tumor-related biomarkers is associated with the tumor growth rate and found that the natural growth of LGGs could be influenced by the expression levels, codeletion, methylation and mutation status of specific tumor biomarkers.

It remains unclear whether a linear growth model or a non-linear growth model is better for evaluating tumor growth. The non-linear growth model is usually based on tumor volumes, whereas the linear growth model is usually based on equivalent tumor diameters (1,2,7,10,23,24,32,33). Most studies quantitatively measuring tumor growth rates have used a linear growth model based on the MTD (1,8-10,12-14,23,24). Although the eVDE in the first

Table 2 Estimated effects of the expression of molecular biomarkers on the growth rate of low-grade gliomas

Molecular biomarker	Subgroup	N	eVDE (mm/year)	Estimated effects (mm/year ± SE)	P value
Ki-67 expression	Low	18	2.6	−0.7±0.4	0.05*
	High	18	1.9		
	N/A	20	1.9		
Mutant p53 expression	Low	22	1.5	3.0±0.4	<0.01*
	High	8	4.5		
	N/A	26	2.0		
TERT promoter type	Wild-type	25	3.4	−1.8±0.3	<0.01*
	Mutant	20	1.6		
	N/A	11	1.5		
1p/19q codeletion status	Non-codeletion	21	3.4	−1.9±0.3	<0.01*
	Codeletion	19	1.4		
	N/A	16	2.2		
EGFR expression	Low	7	2.2	1.8±0.6	<0.01*
	High	9	4.0		
	N/A	40	1.8		
ATRX expression	Low	9	3.6	−2.5±0.4	<0.01*
	High	16	1.1		
	N/A	31	1.9		
MGMT promoter methylation status	Non-methylation	8	5.0	−3.0±0.6	<0.01*
	Methylation	31	2.0		
	N/A	17	1.7		

*, a P value ≤0.05 was considered statistically significant. N/A, not available/data missing; eVDE, equivalent velocity of diameter expansion; SE, standard error.

Table 3 The estimated effect of multiple-factor analysis using the mLMEM

Factor	Estimated effects (mm/year ± SE)	P value
Age	−0.03±0.01	<0.01*
Gender (female *vs.* male)	0.7±0.3	0.51
MGMT promoter (methylation *vs.* non-methylation)	−3.1±0.4	<0.01*
Mutant p53 (high *vs.* low expression)	1.9±0.3	<0.01*
1p/19q (codeletion *vs.* non-codeletion)	−0.5±0.2	0.10
Ki-67 (high *vs.* low expression)	0.4±0.2	0.07
ATRX (high *vs.* low expression)	−1.3±0.4	<0.01*

*, a P value of ≤0.05 was considered statistically significant. mLMEM, multivariate linear mixed effects model; SE, standard error.

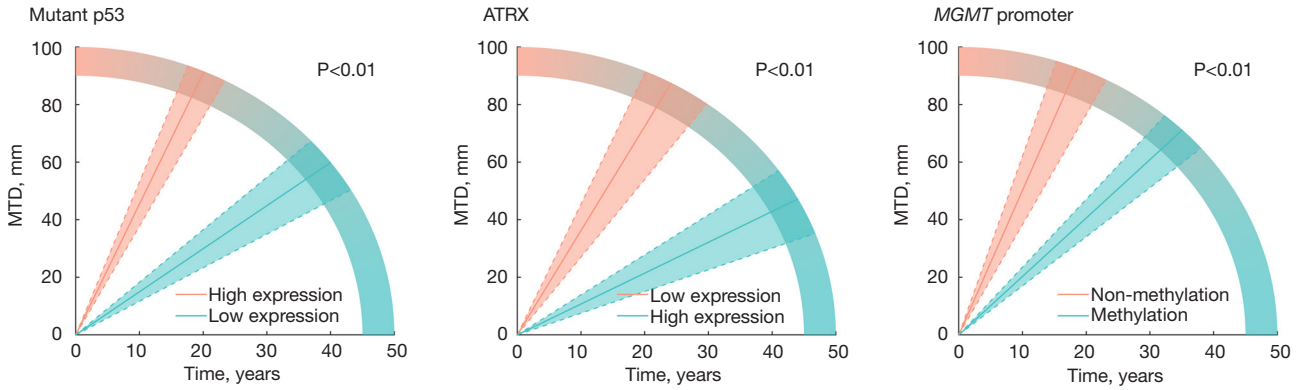

Figure 3 The significant biomarkers in the mLMEM analysis with multifactor analysis and tumor growth in subgroups. Expression levels of mutant p53 and ATRX and *MGMT* promoter methylation had significant effects on the growth rate in the mLMEM analysis. The pink lines and the surrounding fan-shaped areas represent the growth rate and 95% CI of the subgroups with faster growth. The blue lines and the surrounding fan-shaped areas represent the growth rate and 95% CI of the subgroups with slower growth. mLMEM, multivariate linear mixed effects model; CI, confidence interval.

Table 4 The estimated effects of multiple-factor analysis using the mMLEM in the diffuse astrocytoma, *IDH* mutant-type and oligodendroglioma, *IDH* mutant-type subgroups

Molecular biomarker	Estimated effects (mm/year ± SE)	P value
Diffuse astrocytoma, *IDH* mutant-type		
Age	−0.09±0.03	0.01*
Mutant p53 (high *vs.* low expression)	3.6±1.7	0.04*
MGMT promoter (methylation *vs.* non-methylation)	−2.6±0.5	<0.01*
Oligodendroglioma, *IDH* mutant-type		
Age	−0.02±0.006	<0.01*
Gender (female *vs.* male)	0.7±0.2	<0.01*

*, a P value ≤0.05 was considered statistically significant. mLMEM, multivariate linear mixed-effects model; SE, standard error.

study (1) was 4.1 mm/year, calculated using a LMEM, in subsequent studies, the tumor growth rates, which were largely based on the mean or median VDE, were 3.5 to 5.9 mm/year (8,9,12-14,23,24). The growth rate in the pre-surgery linear growth model is only influenced by biological tumor properties. The linear growth model helps clarify whether there are any differences in tumor growth trends among groups with different molecular biomarker statuses, so this model was preferred for assessing tumor growth patterns in the present study.

The regression line of the LMEM indicates the overall trend of the growth of LGGs, and its slope represents the eVDE. In several previous studies (9,10,12-14,24,34), linear regression was used to calculate the growth rate of a tumor in a single patient, while the tumor growth rates in a group of patients were described using the mean or median growth rate. In addition, although the t-test and Wilcoxon test have been used to compare growth rates between groups of gliomas, these methods cannot fully describe the trend of the overall growth for a group of patients, with results easily affected by outliers. An LMEM can be used to avoid the disadvantages mentioned above and exclude the influence of the initial tumor volume; the regression line is a better representation of the overall trend in tumor growth for all patients.

The association between various clinical characteristics and tumor growth rates has been investigated in several previous studies (7-10,24). None of these analyses found an association between the tumor growth rate and age, contrary to our results which showed that age had a

significant impact on the tumor growth rate. Our results indicated that for LGGs, the later the tumor presents, the more slowly it grows, a phenomenon that has been reported for other tumors (35) but needs to be tested in larger data studies. In previous studies, the histological classification of LGGs was not associated with VDE (8,9), which was contrary to our findings, perhaps because the previous studies were conducted before 2021, and their classification standards did not follow the 2021 version of the WHO classification system (4). The growth rate results were consistent with LGG survival for different histological classifications (36). Diffuse astrocytoma, *IDH* mutant-type, grew fastest and was reported to have a shorter survival time, while oligodendroglioma, *IDH* mutant-type, grew the most slowly and was reported to have a longer survival time.

The qualitative influence of molecular biomarkers on tumor growth has previously been investigated (18-21). It is well known that p53 plays an important role in mediating cell proliferation (18,37). A previous study reported that overexpression of mutant p53 led to a significantly faster growth rate than did expression of wild-type p53 (7.7 *vs.* 4.5 mm/year, respectively; P=0.004) (8), consistent with our results. In the present study, expression of ATRX was reported to have a significant impact on tumor growth rate in patients with LGGs, and a low expression of ATRX was significantly associated with a higher eVDE. Although mutation or loss of *ATRX* are associated with a better prognosis in patients with diffuse astrocytoma, *ATRX* mutation or loss are always accompanied by the alternative lengthening of telomeres (ALT) phenotype, which immortalizes the cell (38) and might influence tumor growth. Although *MGMT* promoter methylation status is a well-known indicator associated with drug resistance to alkylating agents (39), the current study indicated that it also had a significant impact on tumor growth, with *MGMT* promoter methylation significantly decreasing the eVDE. Further study is needed to reveal any possible role of *MGMT* promoter methylation in the natural growth of tumors. Previous studies have shown that 1p/19q codeletion significantly decelerates tumor growth rate in LGGs (9,10,14), consistent with the results obtained in our univariate analysis. However, in our multiple-factor analysis, the effect of 1p/19q codeletion was not significant. Therefore, investigations with larger sample sizes are needed in the future to evaluate the individual effects of the 1p/19q codeletion.

Although most important molecular biomarkers for LGGs were analyzed in this study, our limited time span meant that only a few patients with complete data were available for analysis. Furthermore, limited by the retrospective nature of this study, we did not have records of the patients' *CDKN2A/B* status, which is an important indicator for diffuse astrocytoma, *IDH* mutant-type.

According to a previous study (15), fluid-attenuated inversion recovery (FLAIR) imaging shows clearer tumor boundaries, helping to mark tumor regions more accurately. Due to the nature of retrospective studies, a limitation of the current study was that not all patients underwent FLAIR imaging, although they did undergo T2-weighted imaging. To avoid bias from sequence differences, we did not include FLAIR sequence images in the current analysis. 3D FLAIR imaging can increase the resolution of MRI and tumor lesions. We will consider using 3D FLAIR imaging in future studies to increase the robustness of our results. We hope that in future investigations, we can integrate genomics, radiomics, and clinical information to establish the natural growth model of gliomas and provide a clearer understanding of the influences of genetic characteristics on tumor growth.

In conclusion, mutant p53 and ATRX expression levels and *MGMT* promoter methylation were found to be independent factors associated with tumor growth rate in LGGs. High expression level of mutant p53 were found to be significantly associated with a higher tumor growth rate. High expression level of ATRX and *MGMT* promoter methylation were found to be significantly associated with a lower tumor growth rate. Our study used a statistical model to quantitatively identify the effect of molecular biomarkers on the tumor growth rate in LGGs.

Acknowledgments

Funding: This study was supported by National Natural Science Foundation (82072786), Beijing Natural Science Foundation (7174295) and Beijing Hospitals Authority Youth Programme (QML 20170501).

Footnote

Reporting Checklist: The authors have completed the REMARK reporting checklist. Available at https://atm.amegroups.com/article/view/10.21037/atm-21-3998/rc

Data Sharing Statement: Available at https://atm.amegroups.com/article/view/10.21037/atm-21-3998/dss

Peer Review File: Available at https://atm.amegroups.com/article/view/10.21037/atm-21-3998/prf

Conflicts of Interest: All authors have completed the ICMJE uniform disclosure form (available at https://atm.amegroups.com/article/view/10.21037/atm-21-3998/coif). The authors have no conflicts of interest to declare.

Ethical Statement: The authors are accountable for all aspects of the work in ensuring that questions related to the accuracy or integrity of any part of the work are appropriately investigated and resolved. The study was conducted in accordance with the Declaration of Helsinki (as revised in 2013). The study was approved by the Ethics Committee of Beijing Tiantan Hospital (No. KYSB2016-026) and individual consent for this retrospective analysis was waived.

References

1. Mandonnet E, Delattre JY, Tanguy ML, et al. Continuous growth of mean tumor diameter in a subset of grade II gliomas. Ann Neurol 2003;53:524-8.
2. Mandonnet E, Pallud J, Clatz O, et al. Computational modeling of the WHO grade II glioma dynamics: principles and applications to management paradigm. Neurosurg Rev 2008;31:263-9.
3. Cancer Genome Atlas Research Network; Brat DJ, Verhaak RG, et al. Comprehensive, Integrative Genomic Analysis of Diffuse Lower-Grade Gliomas. N Engl J Med 2015;372:2481-98.
4. Louis DN, Perry A, Wesseling P, et al. The 2021 WHO Classification of Tumors of the Central Nervous System: a summary. Neuro Oncol 2021;23:1231-51.
5. Jiang T, Mao Y, Ma W, et al. CGCG clinical practice guidelines for the management of adult diffuse gliomas. Cancer Lett 2016;375:263-73.
6. Harpold HL, Alvord EC Jr, Swanson KR. The evolution of mathematical modeling of glioma proliferation and invasion. J Neuropathol Exp Neurol 2007;66:1-9.
7. Pallud J, Mandonnet E, Duffau H, et al. Prognostic value of initial magnetic resonance imaging growth rates for World Health Organization grade II gliomas. Ann Neurol 2006;60:380-3.
8. Pallud J, Blonski M, Mandonnet E, et al. Velocity of tumor spontaneous expansion predicts long-term outcomes for diffuse low-grade gliomas. Neuro Oncol 2013;15:595-606.
9. Gozé C, Blonski M, Le Maistre G, et al. Imaging growth and isocitrate dehydrogenase 1 mutation are independent predictors for diffuse low-grade gliomas. Neuro Oncol 2014;16:1100-9.
10. Ricard D, Kaloshi G, Amiel-Benouaich A, et al. Dynamic history of low-grade gliomas before and after temozolomide treatment. Ann Neurol 2007;61:484-90.
11. Ribba B, Kaloshi G, Peyre M, et al. A tumor growth inhibition model for low-grade glioma treated with chemotherapy or radiotherapy. Clin Cancer Res 2012;18:5071-80.
12. Blonski M, Pallud J, Gozé C, et al. Neoadjuvant chemotherapy may optimize the extent of resection of World Health Organization grade II gliomas: a case series of 17 patients. J Neurooncol 2013;113:267-75.
13. Pallud J, Llitjos JF, Dhermain F, et al. Dynamic imaging response following radiation therapy predicts long-term outcomes for diffuse low-grade gliomas. Neuro Oncol 2012;14:496-505.
14. Gozé C, Bezzina C, Gozé E, et al. 1P19Q loss but not IDH1 mutations influences WHO grade II gliomas spontaneous growth. J Neurooncol 2012;108:69-75.
15. Pallud J, Taillandier L, Capelle L, et al. Quantitative morphological magnetic resonance imaging follow-up of low-grade glioma: a plea for systematic measurement of growth rates. Neurosurgery 2012;71:729-39; discussion 739-40.
16. Louis DN, Perry A, Reifenberger G, et al. The 2016 World Health Organization Classification of Tumors of the Central Nervous System: a summary. Acta Neuropathol 2016;131:803-20.
17. Lu KV, Chang JP, Parachoniak CA, et al. VEGF inhibits tumor cell invasion and mesenchymal transition through a MET/VEGFR2 complex. Cancer Cell 2012;22:21-35.
18. Michalovitz D, Halevy O, Oren M. Conditional inhibition of transformation and of cell proliferation by a temperature-sensitive mutant of p53. Cell 1990;62:671-80.
19. Deryugina EI, Quigley JP. Matrix metalloproteinases and tumor metastasis. Cancer Metastasis Rev 2006;25:9-34.

20. Jutten B, Rouschop KM. EGFR signaling and autophagy dependence for growth, survival, and therapy resistance. Cell Cycle 2014;13:42-51.
21. Weathers SP, de Groot J. VEGF Manipulation in Glioblastoma. Oncology (Williston Park) 2015;29:720-7.
22. Pallud J, Fontaine D, Duffau H, et al. Natural history of incidental World Health Organization grade II gliomas. Ann Neurol 2010;68:727-33.
23. Peyre M, Cartalat-Carel S, Meyronet D, et al. Prolonged response without prolonged chemotherapy: a lesson from PCV chemotherapy in low-grade gliomas. Neuro Oncol 2010;12:1078-82.
24. Mandonnet E, Pallud J, Fontaine D, et al. Inter- and intrapatients comparison of WHO grade II glioma kinetics before and after surgical resection. Neurosurg Rev 2010;33:91-6.
25. Li Y, Liu X, Qian Z, et al. Genotype prediction of ATRX mutation in lower-grade gliomas using an MRI radiomics signature. Eur Radiol 2018;28:2960-8.
26. Wang Y, Fan X, Zhang C, et al. Identifying radiographic specificity for phosphatase and tensin homolog and epidermal growth factor receptor changes: a quantitative analysis of glioblastomas. Neuroradiology 2014;56:1113-20.
27. Zhang W, Lin Y, Chen B, et al. Recurrent glioblastoma of childhood treated with bevacizumab: case report and molecular features. Childs Nerv Syst 2010;26:137-43.
28. Li S, Jiang T, Li G, et al. Impact of p53 status to response of temozolomide in low MGMT expression glioblastomas: preliminary results. Neurol Res 2008;30:567-70.
29. Yang P, Cai J, Yan W, et al. Classification based on mutations of TERT promoter and IDH characterizes subtypes in grade II/III gliomas. Neuro Oncol 2016;18:1099-108.
30. Zhang CB, Bao ZS, Wang HJ, et al. Correlation of IDH1/2 mutation with clinicopathologic factors and prognosis in anaplastic gliomas: a report of 203 patients from China. J Cancer Res Clin Oncol 2014;140:45-51.
31. Bernal-Rusiel JL, Greve DN, Reuter M, et al. Statistical analysis of longitudinal neuroimage data with Linear Mixed Effects models. Neuroimage 2013;66:249-60.
32. Hlaihel C, Guilloton L, Guyotat J, et al. Predictive value of multimodality MRI using conventional, perfusion, and spectroscopy MR in anaplastic transformation of low-grade oligodendrogliomas. J Neurooncol 2010;97:73-80.
33. Pallud J, Varlet P, Devaux B, et al. Diffuse low-grade oligodendrogliomas extend beyond MRI-defined abnormalities. Neurology 2010;74:1724-31.
34. Pallud J, Mandonnet E, Deroulers C, et al. Pregnancy increases the growth rates of World Health Organization grade II gliomas. Ann Neurol 2010;67:398-404.
35. Huang MS, Kato H, Konaka C, et al. Quantitative cytochemical differences between young and old patients with lung cancer. Chest 1985;88:864-9.
36. Jiang T, Nam DH, Ram Z, et al. Clinical practice guidelines for the management of adult diffuse gliomas. Cancer Lett 2021;499:60-72.
37. Serrano M, Lin AW, McCurrach ME, et al. Oncogenic ras provokes premature cell senescence associated with accumulation of p53 and p16INK4a. Cell 1997;88:593-602.
38. Li F, Deng Z, Zhang L, et al. ATRX loss induces telomere dysfunction and necessitates induction of alternative lengthening of telomeres during human cell immortalization. EMBO J 2019;38:e96659.
39. van Thuijl HF, Mazor T, Johnson BE, et al. Evolution of DNA repair defects during malignant progression of low-grade gliomas after temozolomide treatment. Acta Neuropathol 2015;129:597-607.

Cite this article as: Liu Y, Fan Z, Li S, Liu X, Jiang T, Wang Y, Wang L. Identifying biomarkers associated with tumor growth rate: a longitudinal preoperative magnetic resonance imaging follow-up of low-grade gliomas. Ann Transl Med 2022;10(11):627. doi: 10.21037/atm-21-3998

Supplementary

Table S1 The final cutoff of high expression levels for each biomarker. When we calculated the effect of a biomarker, we analyzed the effects of different high-expression cutoff points (>0, >1, >2, and >3). When the effects of the biomarker expression levels were most significant, the cutoff of the expression level was determined to be the final cutoff point

Biomarker	Number of patients per score					Standard of high expression levels	Estimated effects (High *vs.* low, mm/year ± SE)	P-value
	0	1	2	3	4			
ATRX	9	9	3	1	3	>0	-2.5±0.4	0.16×10^{-8}*
						>1	-2.3±0.4	0.68×10^{-7}
						>2	-1.2±1.2	0.34
						>3	-1.9±1.3	0.16
EGFR	0	0	4	3	9	>0	-	
						>1	-	
						>2	1.0±0.9	0.27
						>3	1.8±0.6	0.003*
Mutant p53	9	7	6	3	5	>0	-0.7±0.7	0.28
						>1	2.4±0.4	0.14×10^{-8}
						>2	3.0±0.4	0.12×10^{-10}*
						>3	2.6±0.5	0.4×10^{-6}
Ki-67	0	18	15	1	2	>0	-	-
						>1	-0.7±0.4	0.05*
						>2	1.7±0.9	0.07
						>3	1.6±1.0	0.10

*, A P-value of the effects of biomarker expression levels was ≤0.05 and most significant. SE, standard error.

Table S2 Comparing the VDE between 2 subgroups (complete or missing molecular data) to assess potential bias from missing data

Molecular biomarker	Number of patients in subgroup		eVDE (mm/year)	Estimated effects (mm/year ± SE)	P-value
Ki-67	Complete	36	2.2	0.2±0.3	0.40
	Missing data	20	1.9		
Mutant p53	Complete	30	2.4	0.5±0.3	0.10
	Missing data	26	2		
TERT promoter	Complete	45	2.3	0.8±0.3	0.02*
	Missing data	11	1.5		
1p/19q	Complete	40	3.4	-0.14±0.4	0.68
	Missing data	16	2.2		
EGFR	Complete	16	3.2	1.4±0.3	<0.01*
	Missing data	40	1.8		
ATRX	Complete	25	2.3	0.3±0.3	0.26
	Missing data	31	1.9		
MGMT promoter	Complete	39	2.1	0.5±0.3	0.10
	Missing data	17	1.7		

*, A P-value ≤0.05 was considered statistically significant. VDE, velocity of diameter expansion; SE, standard error.

https://dx.doi.org/10.21037/atm-21-3998

Table S3 The estimated effect of multiple-factor analysis using the mLMEM in the diffuse astrocytoma, *IDH* mutant subgroup

Molecular biomarker	Estimated effects (mm/year ± SE)	P-value
Age	-0.09±0.03	0.01*
Mutant p53 (High *vs.* low expression)	3.6±1.7	0.04*
MGMT promoter (Methylation *vs.* non-methylation)	-2.6±0.5	< 0.01*

*, A P-value ≤0.05 was considered statistically significant. mLMEM, multivariate linear mixed-effects model; SE, standard error

Table S4 The estimated effect of multiple-factor analysis using the mLMEM in the oligodendroglioma, *IDH* mutant subgroup

Molecular biomarkers	Estimated effects (mm/year ± SE)	P-value
Age	-0.02±0.006	<0.01*
Gender (Female *vs.* male)	0.7±0.2	<0.01*

*, A P-value ≤0.05 was considered statistically significant. mLMEM, multivariate linear mixed-effects model; SE, standard error.

https://dx.doi.org/10.21037/atm-21-3998